Neutron diffraction and scattering study of the weak ferromagnetism in $NaFe_4Sb_{12}$ skutterudite

A. Leithe-Jasper,[1] W. Schnelle,[1] H. Rosner,[1] W. Schweika,[2] and O. Isnard[3,4]

[1]*Max-Planck-Institut für Chemische Physik fester Stoffe, Nöthnitzer Straße 40, 01187 Dresden, Germany*

[2]*Forschungszentrum Jülich, Leo-Brandt-Straße, 52425 Jülich, Germany*

[3]*University Grenoble-Alpes, Institut Néel, 25 Avenue des Martyrs, BP166X, 38042 Grenoble, France*

[4]*CNRS, Institut Néel, 38042 Grenoble, France*

(Received 3 July 2014; revised manuscript received 24 September 2014; published 13 October 2014)

A structural and magnetic investigation of $NaFe_4Sb_{12}$ with filled skutterudite structure is carried out by means of powder neutron diffraction and magnetization measurements in order to investigate the magnetic ground state of this compound. The existence of an ordered magnetic moment on the Fe site of $\approx 0.6\mu_B$/Fe atom is in good agreement with magnetization data. The ratio between the number of spins in the paramagnetic state and in the saturated ferromagnetic state is ≈1.7, indicating some degree of delocalization of the Fe magnetic moment in $NaFe_4Sb_{12}$. Theoretical density-functional calculations of real-space spin-density maps are performed and compared to the experimental findings of weak ferromagnetism in $NaFe_4Sb_{12}$ ($T_C \approx 83$ K). Diffuse magnetic scattering with polarized neutrons revealed that a localized moment exists in the paramagnetic phase which decreases with increasing temperature. The results are discussed in the light of comparison with other intermetallic compounds.

DOI: 10.1103/PhysRevB.90.144416 PACS number(s): 75.50.Bb, 71.20.−b, 75.10.Lp

I. INTRODUCTION

A class of filled skutterudites AFe_4Sb_{12} (A = Na, K, Tl), which surprisingly exhibit a stable ferromagnetic ground state with high Curie temperature T_C of about 85 K, has been discovered a few years ago [1,2]. In these compounds the alkali-metal (or Tl^{1+}) fillers donate one electron to the iron-antimony framework and thus stabilize the ternary crystal structure which is isotypic to the cubic archetype $LaFe_4P_{12}$ [3]. Experimentally, weak ferromagnetism is observed with a small remanent moment of $0.25\mu_B$/Fe atom, which increases dramatically to $0.60\mu_B$/Fe atom in a field of 140 kOe. Thus, the ordered moment is still well below that of a typical ferromagnet as α-iron ($2.22\mu_B$). Electronic structure calculations within the local spin-density approximation (LSDA) have shown that the ferromagnetic state is due to a rather high density of states at E_F from strongly hybridized Fe-Sb states of the iron-antimony host structure and can thus be easily rationalized in view of the Stoner criterion for itinerant ferromagnetism. Observed magnetic susceptibilities of these compounds and the spin-lattice relaxation rate $1/T_1$ measured in nuclear resonance investigations of the ^{23}Na nucleus can be consistently explained with Moriya's self-consistent renormalization (SCF) theory of spin fluctuations [4], which seem to dominate the magnetic properties [2,5]. Additionally, the prevailing quantum spin fluctuations significantly reduce the theoretical LSDA moment ($0.82\mu_B$/Fe atom). In contrast, transfer of more than one electron by other electropositive nonmagnetic filler cations (e.g., alkaline-earth metals, Yb^{2+} or La^{3+}) results in paramagnetic ground states with strongly enhanced susceptibilities at low temperatures [2,6,7]. Moreover, half metallicity of AFe_4Sb_{12} compounds with monovalent fillers predicted by LSDA calculations could be proven experimentally by point-contact Andreev spectroscopy [8]. In these experiments a remarkably high degree of transport spin polarization of up to $P_t = 67\%$ was found.

Up to now, no other kind of transition-metal ferromagnetism has been observed in filled skutterudites and most of the plethora of observed physical properties [9,10], in mainly rare-earth-metal-based compounds, has been attributed to a subtle interplay of the magnetic filler cations and the host structure. From these theoretical and experimental findings the question arose if the magnetic ground state of small ordered magnetic moments and the spin fluctuations observed in bulk magnetic measurements can be probed with neutrons. In addition to the search for an expected small ordered moment in the ferromagnetic ground state by unpolarized neutron diffraction on powder of this material, we further attempted to determine the local moment in the paramagnetic phase by measuring the diffuse magnetic scattering. Therefore, we applied polarized neutrons and polarization analysis in order to separate the magnetic scattering. The experimental results are compared to theoretical density-functional calculation of the real-space spin-density maps.

II. EXPERIMENT

A. Sample preparation

$NaFe_4Sb_{12}$ has been synthesized by powder metallurgical methods from compacted stoichiometric mixtures of $FeSb_2$, NaSb, and Sb powders inside an argon gas glove-box system (oxygen and moisture impurities <1 ppm). Details of the synthesis and sample characterization have been given in our previous publications [1,2]. Low-temperature lattice parameters have been previously refined for $NaFe_4Sb_{12}$ from powder x-ray diffraction on a Guinier-Huber camera with a sample holder incorporated in a closed-cycle helium cryostat [2]. For correct lattice parameter determination the measurement was performed with silicon powder used as an internal standard [11].

B. Neutron diffraction

The refinement of the low-temperature atomic structure has been performed on powder neutron diffraction (ND) data

collected at 2 and 50 K ($\lambda \approx 1.790$ Å; $2\theta_{max} \approx 155^\circ$) at the E9 instrument at the Hahn-Meitner Institute, Berlin, Germany [1].

The ND experiments dedicated to the magnetic structure investigation have been performed at the Institut Laue Langevin (ILL) at Grenoble, France, on the D1B instrument operated by the CNRS at the ILL. During the ND measurements a cylindrical vanadium sample holder of 6 mm inner diameter was used. On the D1B instrument the diffraction patterns have been recorded over an angular range of 80° (2θ) using a multidetector with a step of 0.2° between each of the 400 ^{3}He detection cells. In this configuration D1B is operating with a wavelength of $\lambda = 2.52$ Å selected by a (002) Bragg reflection of a pyrolytic graphite monochromator, the take-off angle being 44.2° in 2θ (for details see Ref. [12]). The measurements were performed at 2, 50, 65, 75, and 95 K using the Orange ILL cryostat. During the refinement of the D1B data, an angular region around 72° (2θ) has been excluded from the analysis due to the presence of a peak originating from the vanadium tail of the cryostat. The data were analyzed with the Rietveld structure refinement program FULLPROF [13]. The definitions for the agreement factors R used in this paper as well as a guideline of the Rietveld refinement procedure can be found elsewhere [14]. The neutron scattering lengths used were $b_{Fe} = 0.945 \times 10^{-12}$ cm, $b_{Sb} = 0.557 \times 10^{-12}$ cm, and $b_{Na} = 0.360 \times 10^{-12}$ cm [15].

The diffuse magnetic scattering experiment with polarization analysis was carried out at the DNS instrument at the Forschungzentrum Jülich, Germany. We used an approximately 2.5 cm^3 sample of $NaFe_4Sb_{12}$ powder for the experiments. The magnetic scattering was separated from nuclear scattering by the so-called xyz-polarization analysis [16]. With this method one measures the spin-flip and non-spin-flip scattering for three different settings of the polarization of the neutron beam along the axes of an orthogonal coordinate system. The x and y axes are in the horizontal scattering plane, and the z axis is perpendicular to it.

C. Calculation procedures

Density-functional calculations have been performed applying the full-potential code FPLO (version FPLO 9.01-35) [17] within the local spin-density approximation using its Perdew-Wang parametrization [18]. A carefully converged k mesh of $20 \times 20 \times 20$ points in the Brillouin zone was used in the self-consistent cycle. In a final step, a $40 \times 40 \times 40$ k mesh had been used for the evaluation of the real-space spin density on a mesh of $100 \times 100 \times 100$ for a crystallographic unit cell.

D. Magnetic properties measurements

The magnetization was measured with a commercial magnetometer (MPMS XL-7, Quantum Design). Isothermal magnetization loops were performed up to external fields of 70 kOe.

III. RESULTS AND DISCUSSION

A. Refinement of the magnetic structure

The powder ND pattern of $NaFe_4Sb_{12}$ recorded at 95 K has been fitted as a nonmagnetic phase ($T_C \approx 83$ K). The

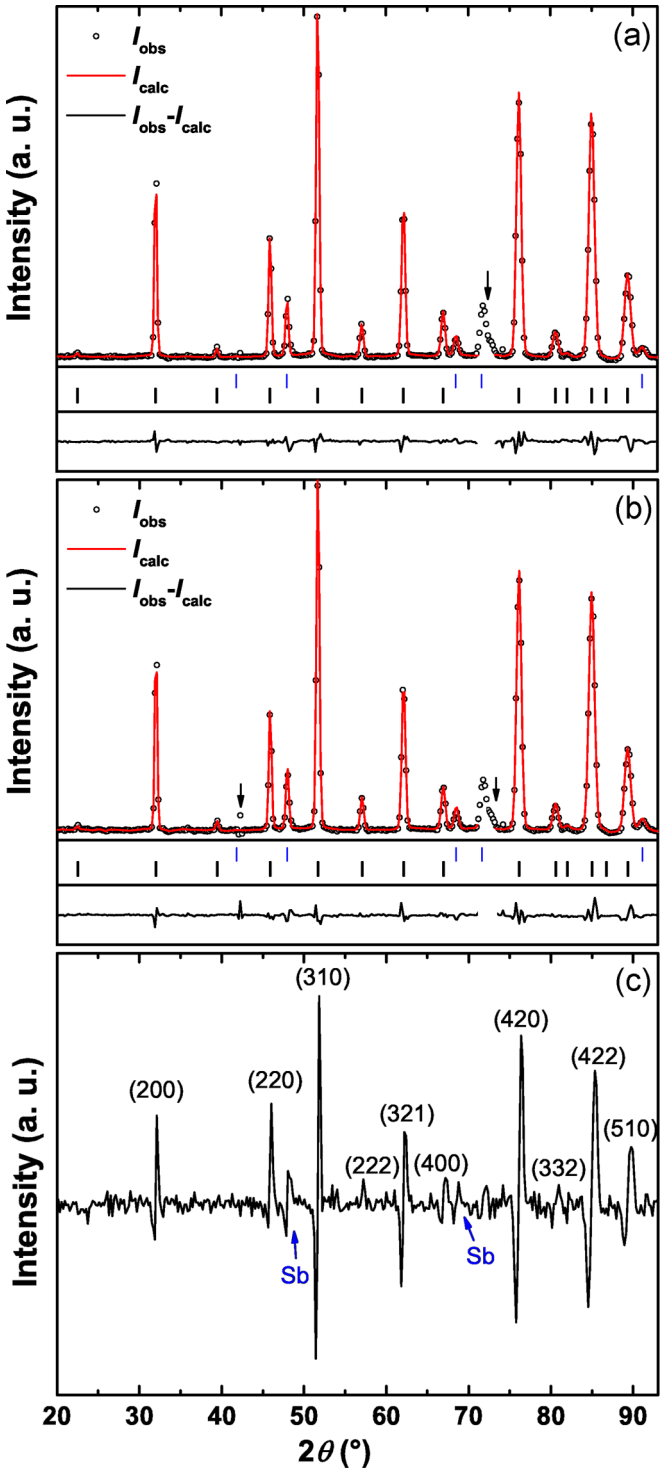

FIG. 1. (Color online) Powder neutron diffraction data of $NaFe_4Sb_{12}$ obtained on the D1B diffractometer: (a) $T = 2$ K, (b) $T = 95$ K. The circles represent experimental data, and the continuous (red) curve the calculated diffractogram. Vertical ticks are the calculated (hkl) reflex positions: upper row (blue) for the Sb impurity, and lower row (black) for $NaFe_4Sb_{12}$. The bottom trace is the difference plot. Arrows indicate artifacts from the sample holder. (c) Difference plot between the patterns recorded at 2 and 95 K, evidencing the diffraction peaks of magnetic origin for $NaFe_4Sb_{12}$.

TABLE I. Structural and magnetic parameters as derived from powder neutron diffraction investigation of $NaFe_4Sb_{12}$ at the indicated temperatures. Space group: $Im\bar{3}$, $Z = 2$. Na is in 2*a* (0,0,0), Fe is in 8*c* (1/4,1/4,1/4), and Sb is in 24*g* (0, 0.6629, 0.8413). Cubic lattice parameter a, isotropic displacement factors B_{iso}, ordered magnetic moment μ_{ord}, and reliability factors R for structural, magnetic, and second phase refinement.

T	a	B_{iso} (Å^2)			μ_{ord}	R values (%)			
(K)	(Å)	Na	Fe	Sb	(μ_B)	p	wp	B	F
95[a]	9.1546(4)	1.57	0.23	0.27	—	11.0	9.77	3.07	2.27
50[b]	9.1529(3)	0.80	0.27	0.23	0.37(23)	7.20	6.90	1.52	1.30
36[c]	9.1526(2)	0.75	0.27	0.23	0.57(15)	7.25	6.72	1.44	1.12
10[d]	9.1523(2)	0.70	0.27	0.23	0.60(10)	7.36	6.98	1.80	1.41
2[e]	9.1523(2)	0.63	0.27	0.23	0.56(20)	10.0	8.23	2.26	1.23

[a]Paramagnetic.
[b]$R_{magn} = 1.07$; second phase Sb: $R_B = 13.5$, $R_F = 9.49$.
[c]$R_{magn} = 0.97$; second phase Sb: $R_B = 14.2$, $R_F = 9.58$.
[d]$R_{magn} = 0.99$; second phase Sb: $R_B = 12.6$, $R_F = 8.69$.
[e]$R_{magn} = 1.62$; second phase Sb: $R_B = 10.5$, $R_F = 7.64$.

obtained fit of the diffraction pattern is shown in Fig. 1(b) and the corresponding structural parameters are summarized in Table I. The sample has been found to be composed of the $NaFe_4Sb_{12}$ filled skutterudite with a small amount of elemental antimony. The temperature-dependent structural data of Sb were fixed to the values found by Fischer *et al.* [19].

It has to be mentioned that the limited Q range (probe on) of this diffraction pattern did not enable us to refine the atomic displacement parameters (ADP), consequently only one of the Na atoms has been refined at 95 K [$B_{iso} = 2.7(8)$ Å^2], whereas those of Fe and Sb have been constrained to the previously refined values of $B_{iso} = 0.27$ Å^2 and $B_{iso} = 0.23$ Å^2, respectively. The large value obtained for the ADP of Na reflects both the thermal displacement and a possible static disorder of the Na atoms in the cage. Such large ADP are well known and common for the filler cations in skutterudite compounds [20,21], in particular those containing light atoms such as Na. For the final refinements we therefore also constrained the temperature factors B_{iso} of Na according to the temperature dependence obtained previously [2].

A comparison of the diffraction patterns recorded at 2, 10, 36, 50, 65, 75, and 95 K, reveals that below the ordering temperature T_C only three Bragg reflections are exhibiting significant magnetic contributions, namely, (200), (220), and (222). Thus, the absence of a substantial change in the diffraction pattern suggests that the magnetic scattering contribution is only small and commensurate with the nuclear lattice. The magnetic contribution is better discerned if one subtracts the 95 K pattern from that recorded at 2 K [see Fig. 1(c)]. For the other Bragg reflections only wavelike signals remain which are characteristic of the thermal change of the lattice parameters. The refinement of the 2 K powder ND pattern is given in Fig. 1(a) and the corresponding structural and magnetic parameters in Table I. In this Rietveld refinement of the $NaFe_4Sb_{12}$ skutterudite, only the Fe site has been considered to carry a magnetic moment and the magnetic form factor used is that of elemental iron. The refined magnetic moment is found to be about $0.56(20)\mu_B$. Neutron data with higher diffraction intensities taken at 10 K allowed a more accurate refinement of the iron moment of $0.60(10)\mu_B$. For ND patterns collected at temperatures exceeding 50 K the refinement of a magnetic moment became unstable. Indeed, the magnetic moment can be considered as the projection of the polarization on the Fe magnetic site but in reality also includes some induced magnetic polarization on the other sites. Such magnetic polarization is expected to be small and cannot be determined from the unpolarized ND pattern recorded here. The small ordered Fe moment results from the large hybridization of the Fe 3*d* states with those of Sb 5*p* as has been reported earlier [1,2].

B. Comparison of theoretical spin-density and observed bulk magnetic properties

To investigate theoretically the distribution of the magnetic moment in the ferromagnetically ordered state we performed density-functional calculations. In agreement with our previous results [1,2,8] we obtain an almost half-metallic ferromagnetic ground state with a moment of $2.98\mu_B$ per formula unit. The magnetic moment is predominantly carried by Fe 3*d* states with a contribution of about $0.86\mu_B$ per Fe site (on-site moment $0.90\mu_B$). The Fe moment is carried mainly by the t_{2g} orbitals (see Fig. 2) of the local coordinate system with respect to the octahedral Sb coordination (see Fig. 3 middle). Due to their high density of states at the Fermi energy, the t_{2g} states should thus dominate the thermodynamic and transport properties of $NaFe_4Sb_{12}$ in the ordered state. Since the Fe 3*d* related magnetism is due to minority spins, the lower lying Sb 5*p* states are weakly polarized in the opposite direction, i.e., parallel to the majority Fe 3*d* spin channel. Sb contributes a magnetic moment of about $-0.04\mu_B$ per Sb site (on-site moment $-0.05\mu_B$). The contribution of Na is minute and only due to overlap.

The small amount of overlap spin density of states between Fe and Sb suggests a rather localized moment distribution. This is confirmed by the calculated real-space spin density (see

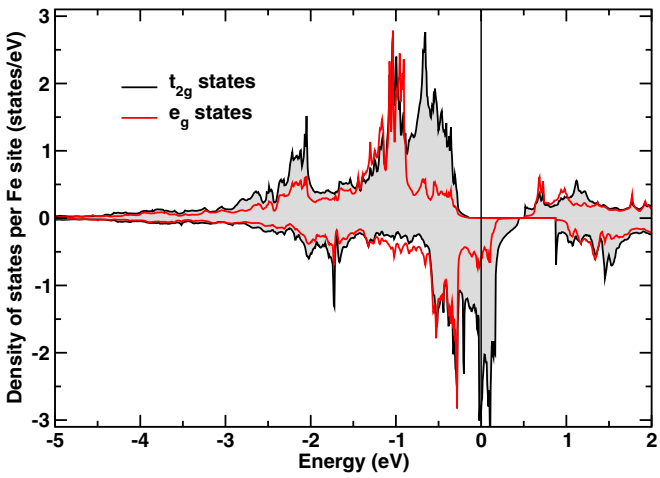

FIG. 2. (Color online) Fe 3*d* orbital-resolved density of states (DOS) of $NaFe_4Sb_{12}$. The three t_{2g} and two e_g orbitals are mutually degenerate. Negative DOS denotes the minority spin contribution.

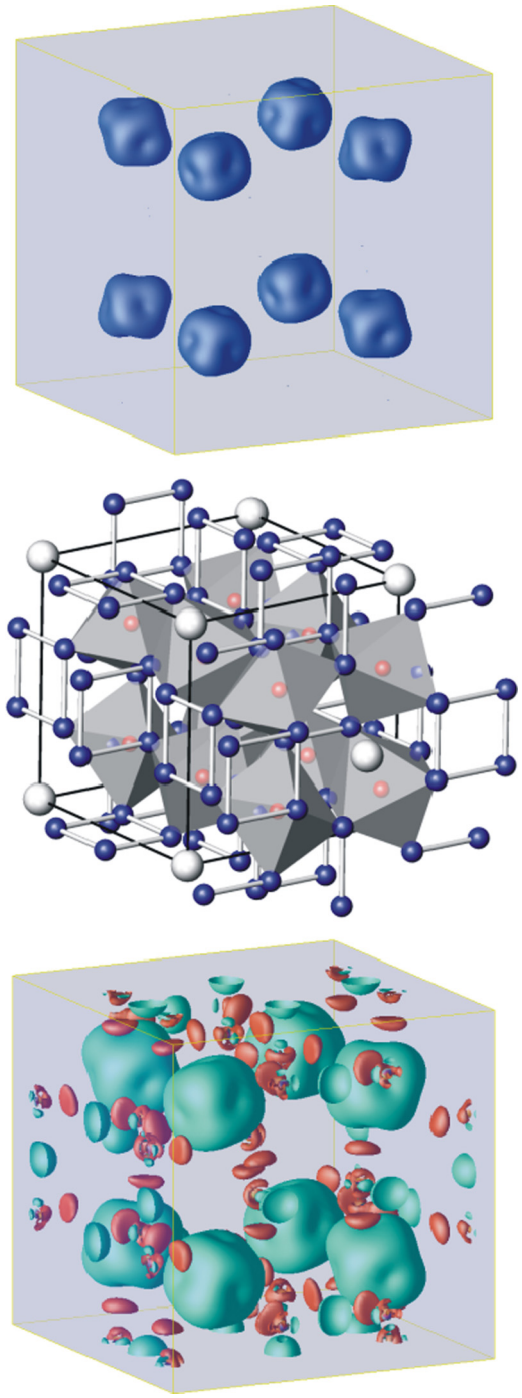

FIG. 3. (Color online) Calculated real-space spin-density maps for $NaFe_4Sb_{12}$. Top: positive spin density, isosurface $0.5\mu_B/Å^3$. Middle: crystal structure of $NaFe_4Sb_{12}$. Large (white) balls: Na; small (blue) balls centering the octahedra: Fe; small (red) balls at octahedral vertices: Sb atoms forming (Sb_4) rectangular units. Bottom: spin-density iso-surface $0.2\mu_B/Å^3$. Large objects (turquoise): positive density; smaller objects (red): negative density.

Fig. 3, top). For larger values of the spin density ($0.5\mu_B/Å^3$), we find a well restricted spatial region that contributes dominantly to the observed ferromagnetism. The shape of the isosurfaces reflects the local symmetry due to the predominant t_{2g} character. Lowering the isovalue to $0.2\mu_B/Å^3$, we still find

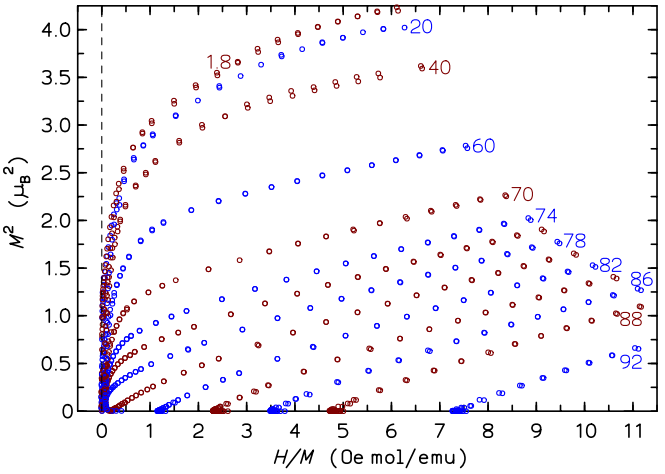

FIG. 4. (Color online) Arrott plot of magnetization isotherms at the indicated temperatures in Kelvin for $NaFe_4Sb_{12}$ (M per formula unit).

good localization around the Fe sites. Simultaneously, we can observe the weak negative polarization of the Sb ligands (see Fig. 3, bottom). Polarization of nonmagnetic antimony atoms was observed in ^{121}Mößbauer spectroscopy [2].

Indeed the magnitude of the Fe magnetic moment has been found to be very sensitive to its local atomic environment, in particular when surrounded by metalloid p elements [22]. As already mentioned, $NaFe_4Sb_{12}$ displays weak ferromagnetic behavior [1,2]. The magnetization of $NaFe_4Sb_{12}$ at 1.8 K (cf. Fig. 7 in Ref. [2]) shows a small hysteresis and only a small remanent moment which can be significantly increased beyond the technical saturation by increasing the external magnetic field. In contrast, strong ferromagnets, such as Co or Ni, show only a negligible increase of the ordered moment with magnetic field after a single domain is formed. It is now interesting to compare the Fe magnetic moment derived from the refinement of the 2, 10, 36, and 50 K neutron data with the thermal variation of the spontaneous magnetization, as obtained from extrapolation of the high field part of Arrott plots for magnetic isotherms at 1.8 K ($0.48\mu_B$/Fe atom), 40 K ($0.44\mu_B$/Fe atom), and 70 K ($0.29\mu_B$/Fe atom) (see Fig. 4). There is a reasonably good correspondence between the refined moments and that obtained from magnetization measurements (considering counterpolarization of other atoms such as Sb) as well as their temperature dependence. Furthermore the obtained magnetic moment at 2 K is also compatible with the band structure calculations (see above), keeping in mind that the theoretical value is expected to be lowered by spin fluctuations. Typical values of coercive field H_C are ranging from 0.6 to 1.2 kOe; the higher H_C values have been obtained for spark plasma sintered samples and the lower for the powder samples. As can be derived from the Arrott plots, the Curie temperature of $NaFe_4Sb_{12}$ is $\approx$83 K.

C. $NaFe_4Sb_{12}$ in the phenomenological context of magnetic order models

According to the high symmetry of the filled skutterudites phases, one can expect the Fe orbital magnetic moment to

be quenched by the crystal electric field. Consequently, the major contribution to the magnetic moment should arise from the spin. Following this hypothesis, the number of spins contributing to the magnetic moment has been determined in the ordered state as well as from the effective magnetic moment determined in the paramagnetic state. For $NaFe_4Sb_{12}$ the paramagnetic susceptibility can be fitted with a Curie-Weiss law and an effective magnetic moment of $1.60\mu_B$ per Fe atom together with a positive Weiss temperature $\theta_W = 87.9$ K is found [2].

The magnetic behavior of the $NaFe_4Sb_{12}$ skutterudites compounds may be analyzed using the self-consistent renormalization theory of spin fluctuations [23,24]. With this model two extreme cases are described: (i) local moment and (ii) exchange enhanced paramagnetism (nearly ferromagnetic). These two extreme cases are characterized by a different value of the ratio $r = S_p/S_0$ between the number of spins determined from the Curie constant (S_p) and the saturation magnetization (S_0) [23,25]. For a local moment we have $r = 1$ while for longitudinal spin fluctuations $r = \infty$. A ratio $r \approx 1.7$ has been calculated here for the $NaFe_4Sb_{12}$ skutterudite. The obtained value is different from ratios r found for ferromagnetic metals with high Curie constants (showing values which are close to 1). Ratios of similar magnitude have been recently found for the weak itinerant ferromagnetic Co-based compounds $Co_3Sn_2S_2$ ($0.29\mu_B$ per Co and with a Curie temperature $T_C = 177$ K) and CoS_2 ($0.85\mu_B$ per Co with $T_C = 120$ K) [26,27]. Indeed, in localized systems, we do not expect the magnitude of the moment to change much when measured below and above T_C, giving a ratio r of unity. In the Rhodes and Wohlfarth plot [25,28,29], the deviation from unity is attributed to an itinerant, i.e., essentially delocalized, magnetic moment [25,28]. Consequently, the use of the r value is a common and useful tool to qualitatively analyze the magnetic behavior of transition-metal-containing intermetallic compounds (see, for instance, Refs. [25,28–31]). The value $r \approx 1.7$ obtained here for $NaFe_4Sb_{12}$ is close to that reported recently for $YFe_{12-x}T_x$ compounds (T = Ti, V, Mo) and actually equal to that of $YFe_{11}Ti$ [32], but significantly larger than the value for α-iron characterized by $r = 1.05$. The obtained value is similar to the values reported for Fe_3C or the one recently found for iron compounds such as $ThFe_{11}C_x$ [33] and $Th_2Fe_{17}C_x$ [34]. In the latter series the r value has been found to be very sensitive to the metalloid concentration, and to decrease when the carbon concentration increases. One can thus expect that the Fe-Sb bond plays a significant role in the itinerancy of the 3d Fe magnetism.

According to the renormalization theory of spin fluctuations [4], the local-moment limit is reached when only the transverse component of local spin fluctuation is important. On the contrary, for a nearly ferromagnetic alloy exhibiting exchange-enhanced paramagnetism, the longitudinal spin fluctuations dominate. Here, the value of the ratio r compared to that of α-Fe indicates that the contribution of the longitudinal spin fluctuations is larger in $NaFe_4Sb_{12}$. In conclusion, the 3d magnetism in the ferromagnetic skutterudites is significantly more delocalized in comparison to α-Fe.

The molecular field coefficient $n_{\text{Fe-Fe}}$ and the effective molecular field or Weiss field H_{eff} can be derived for $NaFe_4Sb_{12}$ assuming that the size of T_C results only from Fe-Fe exchange interactions. $n_{\text{Fe-Fe}}$ is estimated from the magnetic ordering temperature as $n_{\text{Fe-Fe}} = T_C/C$ while H_{eff} is obtained as $H_{\text{eff}} = MT_C/C$ [35,36], where M and C correspond to the magnetization and the Curie constant, respectively. The calculation results in $n_{\text{Fe-Fe}} = 1160\mu_0$ for $NaFe_4Sb_{12}$. The strength of the Fe-Fe exchange coupling corresponds to an exchange field $H_{\text{eff}} = 790$ kOe. Such value of H_{eff} is much smaller than what has been reported for iron-rich phases such as $YFe_{12-x}T_x$ [32].

D. Diffuse scattering of polarized neutrons

Following the above discussion of the magnetic properties of $NaFe_4Sb_{12}$ in both the ordered and paramagnetic state, we will present the results of a diffuse scattering investigation in both magnetic states. The diffuse scattering data with polarized neutrons were taken at four temperatures (300, 90, 60, and 15 K). Below T_C the sample contains ferromagnetic domains that cause a depolarization of the neutron beam. The weak guide fields (approximately 5 Oe at the sample position) for the neutron polarization are too weak to align these domains. Therefore, a separation of the magnetic scattering of the ferromagnetic states by polarization analysis has not been possible. However, the data measured at temperatures above T_C could be separated.

Typical flip ratios are about 1:20 for a reference sample that does not make any spin-flip scattering, which gives an instrumental polarization factor of 90%. As can be seen in Fig. 5 the results for the scattering and, in particular, for the paramagnetic scattering are essentially the same for both data sets taken at 90 and 300 K. The paramagnetic scattering is only about 1/40 or less of the nuclear spin-incoherent scattering for $T = 300$ K as well as for 90 K. The separated nuclear spin-incoherent scattering has been used to quantify the paramagnetic cross section. Compared to a calibration to a vanadium reference, this intrinsic calibration avoids further

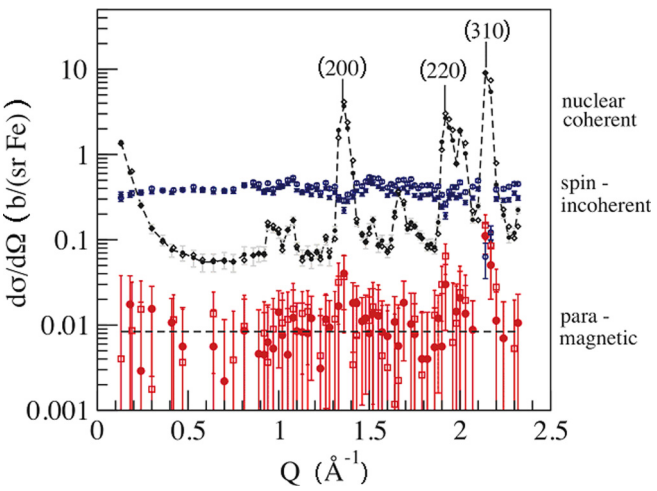

FIG. 5. (Color online) Polarized neutron diffraction and xyz separation of scattering contributions of paramagnetic (red), nuclear coherent (black), and spin-incoherent scattering (blue) of $NaFe_4Sb_{12}$ at 300 K (open) and 90 K (filled symbols). Note the logarithmic scale of absolute intensities.

systematic corrections due to different geometry, absorption properties, etc. The spin-incoherent scattering is essentially given by the contribution from sodium $\sigma_{\text{inc}}(\text{Na}) = 1.62$ barn $(10^{-14}\ \text{m})^2$; hence, the differential spin-incoherent scattering cross section per Fe of 32 mbarn/(sr Fe) yields a calibration of the separated paramagnetic scattering to 8.4 mbarn/sr. This differential cross section corresponds to a local moment of only $0.06\mu_B$ and indicates that the moment is even significantly weaker in the disordered phase. Considering only statistical errors from the neutron counts an upper limit would be $(0.06 + 0.06)\mu_B$. Note that, different from Bragg diffraction determining the ordered moment S_z along a quantization axis, the diffuse paramagnetic scattering integrated in energy is given by the modulus $S(S+1)$, related to the sum of longitudinal spin relaxations and damped transverse spin excitations. The paramagnetic signal is quasielastic and its width in energy is determined by the strength of the exchange coupling and thermal energies. Indeed, it can be expected that not the whole paramagnetic scattering has been integrated by diffraction, particularly in view of the relative long wavelength and small incoming neutron energy. However, assuming that the low-temperature local moment of $0.6\mu_B$ would be persistent in the disordered phase, one would have to conclude that 90% of the intensity is out of the accepted energy range of about 10 meV. This seems to be far beyond the possible losses by diffraction integration on this experiment. A more realistic estimate is that the local moment in the disordered phase is smaller by at least a factor of 3 than the ground-state local moment. Note also the unpolarized ND data indicates that the Fe moment decreases with temperature within the ordered phase. Therefore, we may conclude that the local moment of Fe in $NaFe_4Sb_{12}$ skutterudite decreases with temperature. To address this further, more precise energy-resolved measurements of the paramagnetic scattering seem to be of particular interest for future investigations.

IV. SUMMARY

The structural and magnetic properties of the filled skutterudite $NaFe_4Sb_{12}$ has been studied experimentally by means of combining powder neutron diffraction investigation, magnetic measurements, as well as diffuse magnetic scattering with polarized neutrons. Powder neutron diffraction showed the existence of an ordered magnetic moment on the Fe site of $\approx 0.6\mu_B$/Fe atom in good agreement with magnetization data at low temperature. A value of 1.7 is obtained for the ratio between the number of spins in the paramagnetic state and in the saturated ferromagnetic state indicating some degree of delocalization of the Fe magnetic moment in $NaFe_4Sb_{12}$ compared with elemental iron. Theoretical calculations of real-space spin-density maps corroborate the experimental findings of a predominately localized weak ferromagnetism in $NaFe_4Sb_{12}$. Diffuse magnetic scattering with polarized neutrons, taken at 90 and 300 K, revealed that a localized moment exists in the paramagnetic phase and decreases with increasing temperature.

ACKNOWLEDGMENTS

The authors thank Yuri Grin for continuous support. We warmly thank the CNRS-CRG instrument group and the Institut Laue Langevin for providing the neutron beamtime on the D1B instrument.

[1] A. Leithe-Jasper, W. Schnelle, H. Rosner, N. Senthilkumaran, A. Rabis, M. Baenitz, A. Gippius, E. Morozova, J. A. Mydosh, and Y. Grin, Phys. Rev. Lett. **91**, 037208 (2003); **93**, 089904 (2004).

[2] A. Leithe-Jasper, W. Schnelle, H. Rosner, M. Baenitz, A. Rabis, A. A. Gippius, E. N. Morozova, H. Borrmann, U. Burkhardt, R. Ramlau, U. Schwarz, J. A. Mydosh, Y. Grin, V. Ksenofontov, and S. Reiman, Phys. Rev. B **70**, 214418 (2004).

[3] W. Jeitschko and D. Braun, Acta Crystallogr., Sect. B: Struct. Sci. **33**, 3401 (1977).

[4] T. Moriya, *Spin Fluctuations in Itinerant Electron Magnetism* (Springer-Verlag, Berlin, 1985).

[5] A. Gippius, M. Baenitz, E. Morozova, A. Leithe-Jasper, W. Schnelle, A. Shevelkov, E. Alkaev, A. Rabis, J. Mydosh, Y. Grin, and F. Steglich, J. Magn. Magn. Mater. **300**, e403 (2006).

[6] T. Takabatake, E. Matsuoka, S. Narazu, K. Hayashi, S. Morimoto, T. Sakakawa, K. Umeo, and M. Sera, Physica B **383**, 93 (2006).

[7] W. Schnelle, A. Leithe-Jasper, M. Schmidt, H. Rosner, H. Borrmann, U. Burkhardt, J. A. Mydosh, and Y. Grin, Phys. Rev. B **72**, 020402(R) (2005).

[8] G. Sheet, H. Rosner, S. Wirth, A. Leithe-Jasper, W. Schnelle, U. Burkhardt, J. A. Mydosh, P. Raychaudhuri, and Y. Grin, Phys. Rev. B **72**, 180407(R) (2005).

[9] C. Uher, Semicond. Semimetals **69**, 139 (2001).

[10] B. C. Sales, in *Handbook on the Physics and Chemistry of Rare Earths*, edited by K. A. Gschneidner, Jr., J.-C. G. Bünzli, and V. K. Pecharsky (Elsevier, Amsterdam, 2003), Vol. 33, Chap. 211, pp. 1–34.

[11] G. K. White and M. L. Minges, Int. J. Thermophys. **18**, 1269 (1997).

[12] The Yellow Book, www.ill.fr.

[13] J. Rodríguez-Carvajal, Physica B **192**, 55 (1993).

[14] L. B. McCusker, R. B. Von Dreele, D. E. Cox, D. Louer, and P. Scardi, J. Appl. Crystallogr. **32**, 36 (1999).

[15] V. F. Sears, Neutron News **3**, 26 (1992).

[16] O. Schärpf and H. Capellmann, Phys. Status Solidi A **135**, 359 (1993).

[17] K. Koepernik and H. Eschrig, Phys. Rev. B **59**, 1743 (1999).

[18] J. P. Perdew and Y. Wang, Phys. Rev. B **45**, 13244 (1992).

[19] P. Fischer, I. Sosnowska, and M. Szymanski, J. Phys. C: Solid State Phys. **11**, 1043 (1978).

[20] B. C. Sales, B. C. Chakoumakos, D. Mandrus, and J. W. Sharp, J. Solid State Chem. **146**, 528 (1999).

[21] W. Schnelle, A. Leithe-Jasper, H. Rosner, R. Cardoso-Gil, R. Gumeniuk, D. Trots, J. A. Mydosh, and Y. Grin, Phys. Rev. B **77**, 094421 (2008).

[22] O. Isnard and D. Fruchart, J. Alloys Compd. **205**, 1 (1994).

[23] T. Moriya, J. Magn. Magn. Mater. **14**, 1 (1979).
[24] T. Moriya, J. Magn. Magn. Mater. **100**, 261 (1991).
[25] P. Rhodes and E. P. Wohlfarth, Proc. R. Soc. Lond. A **273**, 247 (1963).
[26] T. Kubodera, H. Okabe, Y. Kamihara, and M. Matoba, Physica B **378–380**, 1142 (2006).
[27] M. Holder, Y. S. Dedkov, A. Kade, H. Rosner, W. Schnelle, A. Leithe-Jasper, R. Weihrich, and S. L. Molodtsov, Phys. Rev. B **79**, 205116 (2009).
[28] J. Kübler, *Theory of Itinerant Electron Magnetism* (Oxford Science Publications, Oxford, 2000).
[29] K. Shimizu, H. Maruyama, H. Yamazaki, and H. Watanabe, J. Phys. Soc. Jpn. **59**, 305 (1990).
[30] E. Burzo, J. Magn. Magn. Mater. **196–197**, 901 (1999).
[31] E. Burzo, J. Magn. Magn. Mater. **140–144**, 2013 (1995).
[32] O. Isnard and V. Pop, J. Phys.: Condens. Matter **21**, 406003 (2009).
[33] O. Isnard, V. Pop, and K. H. J. Buschow, J. Magn. Magn. Mater. **256**, 133 (2003).
[34] O. Isnard, V. Pop, and K. H. J. Buschow, J. Appl. Phys. **101**, 103908 (2007).
[35] J. J. M. Franse and R. J. R. Radwanski, in *Handbook of Magnetic Materials*, edited by K. H. J. Buschow (North Holland, Amsterdam, 1993), Vol. 7, p. 344.
[36] K. H. J. Buschow and F. R. de Boer, *Physics of Magnetism and Magnetic Materials* (Kluwer, New York, 2003).